and the time scales for bifurcation into physical and chemical channels underscore the critical importance of structural dynamics in determining the true nature of complex molecular behaviors and the energy landscapes of radiationless transitions.

References and Notes

1. E. C. Lim, Ed., *Molecular Luminescence* (Benjamin, New York, 1969).
2. E. C. Lim, *Adv. Photochem.* **23**, 165 (1997).
3. J. D. Baldwin, in *Reactive Intermediate Chemistry*, R. A. Moss, M. S. Platz, M. Jones, Eds. (Wiley, New York, 2004), p. 899.
4. E. C. Friedberg, *Nature* **421**, 436 (2003).
5. C. E. Crespo-Hernandez, B. Cohen, P. M. Hare, B. Kohler, *Chem. Rev.* **104**, 1977 (2004).
6. B. R. Henry, M. Kasha, *Annu. Rev. Phys. Chem.* **19**, 161 (1968).
7. G. W. Robinson, R. P. Frosch, *J. Chem. Phys.* **38**, 1187 (1963).
8. M. Bixon, J. Jortner, *J. Chem. Phys.* **48**, 715 (1968).
9. J. Michl, in *Conical Intersections: Electronic Structure, Dynamics and Spectroscopy*, W. Domcke, D. R. Yarkony, H. Koppel, Eds. (World Scientific, Singapore, 2004), p. ix.
10. G. B. Kistiakowsky, C. S. Parmenter, *J. Chem. Phys.* **42**, 2942 (1965).
11. K. B. Eisenthal, Ed., *Applications of Picosecond Spectroscopy to Chemistry* (Reidel, Boston, 1984).
12. A. H. Zewail, in *Les Prix Nobel: The Nobel Prizes 1999*, T. Frängsmyr, Ed. (Almqvist & Wiksell, Stockholm, 2000), pp. 103–203.
13. H. Ihee *et al.*, *Science* **291**, 458 (2001).
14. R. Srinivasan, V. A. Lobastov, C.-Y. Ruan, A. H. Zewail, *Helv. Chim. Acta* **86**, 1763 (2003).
15. C.-Y. Ruan, F. Vigliotti, V. A. Lobastov, S. Y. Chen, A. H. Zewail, *Proc. Natl. Acad. Sci. U.S.A.* **101**, 1123 (2004).
16. C.-Y. Ruan, V. A. Lobastov, F. Vigliotti, S. Y. Chen, A. H. Zewail, *Science* **304**, 80 (2004).
17. J. M. Thomas, *Angew. Chem. Int. Ed. Engl.* **43**, 2606 (2004).
18. J. H. Callomon, J. E. Parkin, R. Lopez-Delgado, *Chem. Phys. Lett.* **13**, 125 (1972).
19. V. A. Lobastov *et al.*, *J. Phys. Chem. A* **105**, 11159 (2001).
20. E. Villa, A. Amirav, E. C. Lim, *J. Phys. Chem.* **92**, 5393 (1988).
21. I. Yamazaki *et al.*, *Chem. Phys. Lett.* **92**, 421 (1982).
22. D. P. Zhong *et al.*, *Chem. Phys. Lett.* **298**, 129 (1998).
23. K. A. Prather, Y. T. Lee, *Isr. J. Chem.* **34**, 43 (1994).
24. K. E. Wilzbach, D. J. Rausch, *J. Am. Chem. Soc.* **92**, 2178 (1970).
25. M. Chachisvilis, A. H. Zewail, *J. Phys. Chem. A* **103**, 7408 (1999).
26. O. L. Chapman, C. L. McIntosh, J. Pacansky, *J. Am. Chem. Soc.* **95**, 614 (1973).
27. D. E. Johnstone, J. R. Sodeau, *J. Phys. Chem.* **95**, 165 (1991).
28. S. Kudoh, M. Takayanagi, M. Nakata, *J. Photochem. Photobiol. A* **123**, 25 (1999).
29. A. L. Sobolewski, W. Domcke, *Chem. Phys. Lett.* **180**, 381 (1991).
30. Although it is conceivable that the hot ground-state molecules could undergo further ring-opening reaction, our one-photon energy of ~107 kcal/mol is inadequate for complete C–N bond scission on the ground state. Furthermore, cleavage via this mechanism is known to proceed via initial loss of the α-hydrogen atom to form the pyridyl radical (*44*); however, there is minimal loss of hydrogen observed in pyridine upon photoexcitation (*23*).
31. I. Yamazaki, K. Sushida, H. Baba, *J. Chem. Phys.* **71**, 381 (1979).
32. I. Yamazaki, K. Sushida, H. Baba, *J. Lumin.* **18–9**, 425 (1979).
33. I. Yamazaki, T. Murao, T. Yamanaka, K. Yoshihara, *Faraday Discuss.* **75**, 395 (1983).
34. J. W. Pavlik, N. Kebede, M. Thompson, A. C. Day, J. A. Barltrop, *J. Am. Chem. Soc.* **121**, 5666 (1999).
35. J. W. Pavlik, personal communication.
36. S. Kudoh, M. Takayanagi, M. Nakata, *Chem. Phys. Lett.* **308**, 403 (1999).
37. S. Porcinai, P. Foggi, *Nuovo Cimento Soc. Ital. Fis. D* **19**, 889 (1997).
38. Y. Hirata, E. C. Lim, *J. Chem. Phys.* **72**, 5505 (1980).
39. M. Berger, I. L. Goldblatt, C. Steel, *J. Am. Chem. Soc.* **95**, 1717 (1973).
40. U. Brühlmann, M. Nonella, P. Russegger, J. R. Huber, *Chem. Phys.* **81**, 439 (1983).
41. N. Ohmori, T. Suzuki, M. Ito, *J. Phys. Chem.* **92**, 1086 (1988).
42. A. V. Polevoi, V. M. Matyuk, G. A. Grigor'eva, V. K. Potatov, *Khim. Vys. Energ.* **18**, 195 (1984).
43. C. R. Silva, J. P. Reilly, *J. Phys. Chem. A* **101**, 7934 (1997).
44. R. Liu, T. T.-S. Huang, J. Tittle, D. Xia, *J. Phys. Chem. A* **104**, 8368 (2000).

45. Supported by NSF and the U.S. Air Force Office of Scientific Research.

Supporting Online Material
www.sciencemag.org/cgi/content/full/1107291/DC1
Figs. S1 and S2

9 November 2004; accepted 21 December 2004
Published online 6 January 2005;
10.1126/science.1107291
Include this information when citing this paper.

Electron Spectroscopy of Aqueous Solution Interfaces Reveals Surface Enhancement of Halides

Sutapa Ghosal,[1,2] John C. Hemminger,[1]* Hendrik Bluhm,[3] Bongjin Simon Mun,[4] Eleonore L. D. Hebenstreit,[2] Guido Ketteler,[2] D. Frank Ogletree,[2] Felix G. Requejo,[2,5] Miquel Salmeron[2]

It has been suggested that enhanced anion concentrations at the liquid/vapor interface of airborne saline droplets are important to aerosol reactions in the atmosphere. We report ionic concentrations in the surface of such solutions. Using x-ray photoelectron spectroscopy operating at near ambient pressure, we have measured the composition of the liquid/vapor interface for deliquesced samples of potassium bromide and potassium iodide. In both cases, the surface composition of the saturated solution is enhanced in the halide anion compared with the bulk of the solution. The enhancement of anion concentration is more dramatic for the larger, more polarizable iodide anion. By varying photoelectron kinetic energies, we have obtained depth profiles of the liquid/vapor interface. Our results are in good qualitative agreement with classical molecular dynamics simulations. Quantitative comparison between the experiments and the simulations indicates that the experimental results exhibit more interface enhancement than predicted theoretically.

A detailed knowledge of halide ion concentrations at solution interfaces is of great importance for understanding the chemistry of salt solutions. This is of current interest because halide ion concentrations play a key role in many atmospheric and environmental chemistry processes. For example, reactions of sea-salt aerosols with gas-phase oxidants such as OH and ozone have been suggested as a mechanism for the introduction of substantial amounts of gas-phase chlorine and bromine compounds into the marine troposphere (*1*, *2*). Recent field measurements have directly observed Cl_2, Br_2, and BrCl, which provides strong evidence that halogen compounds are indeed important in the chemistry of the troposphere, both at midlatitude and in polar regions (*3*–*8*).

Studies of the reactivity of salt solutions have suggested that there is an enhancement of the absolute anion concentrations at the interface. At first sight, such an enhancement appears contrary to thermodynamic expectations, because image-charge repulsion should move ions away from the surface and because the addition of salt to water causes an increase in surface tension. Hu *et al*. (*9*) suggested that Cl^- and Br^- ions must exist at the liquid/vapor interface of such solutions based on measurements of the uptake of Cl_2 and Br_2 gases by alkali-halide salt solutions. To explain experimental measurements of reactions of gas-phase oxidants with concentrated NaCl aerosol droplets, Knipping *et al*. (*1*) have also suggested that Cl^- ion concentrations are enhanced at the liquid/vapor interface. This contention is supported by classical molecular dynamics (MD) simulations. More recently, Jungwirth and Tobias (*10*, *11*) have elaborated on the classical MD simulations, providing additional theoretical evi-

[1]Department of Chemistry, University of California, Irvine, CA 92697, USA. [2]Materials Sciences Division, Lawrence Berkeley National Laboratory, Berkeley, CA 94720, USA. [3]Chemical Science Division, Lawrence Berkeley National Laboratory, Berkeley, CA 94720, USA. [4]Advanced Light Source, Lawrence Berkeley National Laboratory, Berkeley, CA 94720, USA. [5]Departamento de Física, Facultad de Ciencias Exactas, Universidad Nacional de La Plata, 1900 La Plata, Argentina.

*To whom correspondence should be addressed. E-mail: jchemmin@uci.edu

dence for the existence of enhanced concentrations of the larger, more polarizable halogen ions at the surfaces of the corresponding aqueous solutions. Their simulations are consistent with the observed changes in surface tension with salt concentration (*10*).

Garrett (*12*) recently pointed out that "direct experimental observations of molecular structure and energetics of ions in the interfacial region are needed to corroborate the simulations." Given both the fundamental and the atmospheric importance of the surface chemistry at the liquid/vapor interface of salt solutions, a number of laboratories have applied surface-sensitive experimental probes to shed light on the subject of surface ion concentrations in salt solutions. Nonlinear optical experiments, particularly second-harmonic generation (SHG) and vibrational sum-frequency generation (VSFG), have been shown to probe interfacial properties. Allen and co-workers (*13*) have used a combination of conventional Raman spectroscopy and VSFG to compare the infrared spectra from the bulk of salt solutions (Raman spectra) with spectra from the surface region (the VSFG spectra). The VSFG experiments are sensitive to the region of the sample near the surface that is noncentrosymmetric. They interpret their results to show that the noncentrosymmetric region of the solution extends farther into the bulk for the bromide and iodide salt solutions than for pure water. The enhanced disruption of the molecular symmetry when going farther into the bulk is consistent with the classical MD simulations, which show that bromide and iodide ions are enhanced near the surface, with a corresponding enhancement of the cation just below the surface (*10*, *13*).

Raymond *et al.* (*14*) carried out isotopic dilution experiments in conjunction with the VSFG technique. The isotopic dilution experiments provide an elegant way to separate contributions from different species to the complex OH stretching region of the VSFG spectrum. Their results on alkali-halide solutions are consistent with the existence of anions in the near-surface region of the solution. However, they do not see any change in the hydrogen bonding of the surface water that would imply either enhanced halide ion concentrations near the surface or the separation of anions and cations in the near-surface region.

Petersen *et al.* (*15*) recently reported resonant SHG experiments in which they probed the surface region of NaI and KI solutions over a wide range of concentrations. Over a narrow range of low concentrations (millimolar), they showed that their results are consistent with an enhanced anion concentration in the surface region probed by the SHG experiment.

Weber *et al.* (*16*) reported valence-band photoemission experiments in which they were able to probe the surface region of a liquid jet of alkali-halide solution. In their experiments, the liquid jet is in contact with a vacuum and thus is not in equilibrium with the vapor of the solution. Although their results do not necessarily support any surface excess of anions as predicted by the classical MD simulations, they are at the same time unable to rule out the existence of such an enhancement given the particulars of their experiment. However, based on the observed change in photoemission signals as a function of the concentration of the solution used to generate the liquid jet, they suggest that there is a "negative surface excess" of ions for the case of NaI solutions—in apparent contradiction with the classical MD simulations.

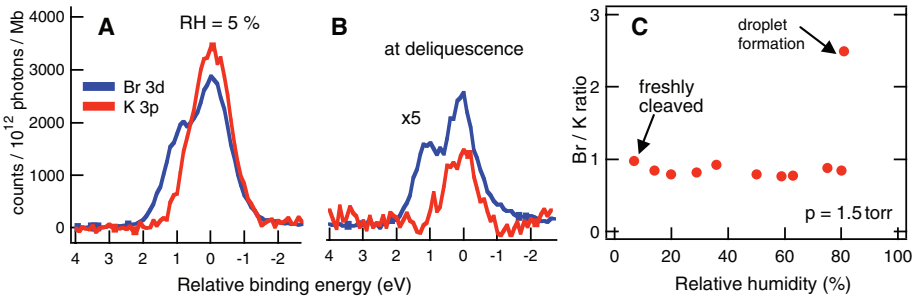

Fig. 1. Br 3d and K 3p core-level photoemission spectra acquired (**A**) at a relative humidity (RH) of 5% and (**B**) at the deliquescence point. The photon energy is adjusted so that both peaks have the same kinetic energy, 160 eV. The count rate is normalized to incident photon flux and photoemission cross section for each element. At RH = 5%, the measured ratio is Br/K = 1.1:1, close to the expected value of 1. At deliquescence there is a factor 2 enhancement of Br with respect to K (Br/K = 2.5:1). (**C**) The Br/K ratio as a function of water vapor relative humidity. Br/K ratio is virtually constant until deliquescence is reached.

We have directly measured the ion concentrations in the surface region of alkali-halide aqueous solutions by using x-ray photoelectron spectroscopy (XPS) to profile the surface composition of an alkali-halide salt in contact with water vapor. The recent development of techniques to acquire photoemission spectra in gas environments at pressures up to several torr (*17*) has allowed us to study an alkali-halide sample as a function of water vapor pressure, starting with the freshly cleaved, dry sample up to the deliquescence point of the salts (*18*). Relative humidity was varied by holding the sample at –10°C while varying the water pressure or by maintaining the pressure at ~2 torr while varying the sample temperature. In the experiments, the K 2p and 3p, the O 1s, and the C 1s peaks were monitored, as well as the Br 3d and I 4d peaks for KBr and KI, respectively. The C 1s peaks were monitored to quantify the small amount (submonolayer) of carbonaceous material that will always be present in such liquid/vapor interface studies. Charging of the salt surface was compensated by photoelectrons from ionized water vapor.

Quantification of the photoemission data are challenging because both gas-phase attenuation and transmission through the electron optics are energy-dependent. We overcome this problem by measuring relative anion/cation/oxygen signals for identical photoelectron kinetic energies (KEs), obtained by choosing appropriate x-ray excitation energies and normalizing by the corresponding ionization cross sections [taken from Yeh and Lindau (*19*)]. The use of the same KE also ensures that the sample depth analyzed is the same for all of the elements. The energy-dependent x-ray flux was measured using a calibrated photodiode. Radiation damage from the incident x-rays was avoided by continuously displacing the sample so that the spectra are obtained in fresh spots of the sample.

The change in the surface Br/K atom ratio as a function of relative humidity is shown in Fig. 1 from an experiment in which a KBr single crystal sample was cleaved in vacuum. The XPS spectra were then obtained for different values of the water vapor relative humidity up to deliquescence of the sample, at which point a visible droplet formed at the surface. These data are typical of the results obtained in a number of experiments involving different KBr samples and in two separate analysis chambers. The spectra in Fig. 1, A and B, were obtained from a sample that was cleaved just before introduction into the vacuum system and correspond to a photoelectron KE of 160 eV. The Br/K ratio remains constant around an average value of 0.8 ± 0.1 as the water vapor pressure is increased below the deliquescence point. In the saturated solution formed at deliquescence, a significant increase of the Br/K ratio to 2.5 ± 0.2 was observed. The results were independent of the manner in which the relative humidity was varied (i.e., by varying the water vapor pressure at constant sample temperature or by varying the sample temperature at constant water pressure).

For KI, a similar abrupt change was observed from an I/K ratio of 1 below deliquescence to a value of 3.4 ± 0.2 at deliquescence. These results, along with the concentration of water, obtained using the O 1s peak, are summarized in Fig. 2. Using the O peak intensity, we obtained absolute concentration values. The values are Br/K/O(H_2O) = 15:7:78 and I/K/O(H_2O) = 25:8:67. The

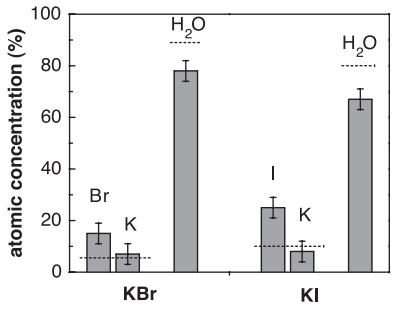

Fig. 2. Atomic concentration at the deliquescence point. The kinetic energy of the photoelectrons was 200 eV, corresponding to an escape depth of two to three atomic layers. Error bars indicating standard deviations are shown for the experimental measurements. The dashed lines indicate the expected concentrations of ions and water molecules from thermodynamic data for bulk, saturated solutions.

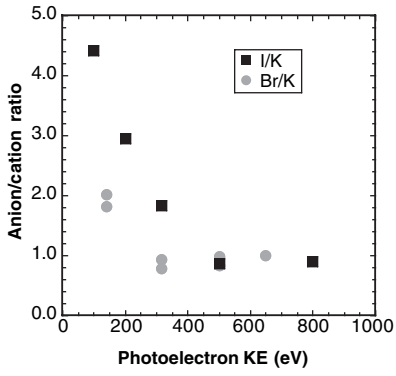

Fig. 3. Measured anion/cation atomic ratio as a function of the photoelectron kinetic energy. The circles are the measured Br/K ratios for KBr. The squares are the values of I/K for KI.

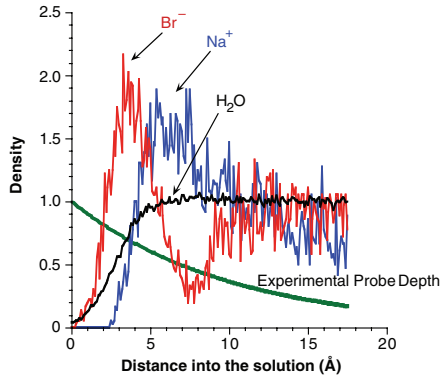

Fig. 4. Results from classical MD simulations (*10*, *11*) of a 1.2 M NaBr solution, showing the predicted enhancement of the halide ion at the interface. An example of the experimental probe depth function for the case of an electron IMFP of 10 Å is included for comparison.

values expected for a saturated solution in the absence of ion segregation effects can be obtained from data on salt solubility at the appropriate temperature (*20*). In the absence of segregation, the ratios at –10°C are expected to be Br/K/O(H_2O) = 5.5:5.5:84 and I/K/O(H_2O) = 10:10:80. Thus, as shown in Fig. 2, there is an enhancement of the absolute anion concentrations at the interface in addition to an enhanced interfacial anion/cation ratio.

The depth into the sample probed by XPS is determined by the inelastic scattering of the electrons as they exit the sample. Electrons that undergo inelastic scattering contribute to the spectral background and are lost from the peak signal. The inelastic mean free path (IMFP) of electrons is a function of their KE, so it is possible to determine concentration depth profiles by monitoring the same elements with different photon energies (and thus different photoelectron KEs). For KEs above 100 eV, the IMFP increases with energy. Results from such experiments for deliquesced KBr and KI samples are shown in Fig. 3, in which we plot the measured anion/cation atomic ratio as a function of the photoelectron KE. Both KI and KBr show significant enhancement of the halide ion concentration in the more surface-sensitive experiments (low photoelectron KE). In both cases, a ratio of 1 (±0.1) was obtained when the experiment was performed with photoelectrons of higher KE that probe deeper into the solution.

Our results therefore agree qualitatively with the picture derived from the MD simulations, not only in regard to the preferential enhancement of anion concentration at the surface but also in confirming the greater effect for the larger, more polarizable iodide. A more quantitative comparison between our experiments and the simulations requires a convolution of the simulation results with an exponentially decaying experimental probe depth that would be characteristic of the XPS experiment (*21*). Figure 4 shows the results of the simulations for a 1.2 M NaBr solution carried out by Jungwirth and Tobias, along with an exponentially decaying experimental probe depth function for the case of an electron IMFP of 10 Å. Unfortunately, the IMPF values are not well known, particularly for liquids such as water. In the case of solid materials, reported values of IMPF vary from 5 to 10 Å at electron KEs in the range from 100 to 200 eV (*22*). Using these two extreme values and the density profiles of the Jungwirth and Tobias simulations (*10*, *11*), we obtain predicted anion/cation ratios of I^-/cation = 1.65 (IMPF = 5.0 Å) and 1.26 (IMPF = 10 Å) and Br^-/cation = 1.32 (IMPF = 5.0 Å) and 1.10 (IMPF = 10 Å). It appears then that the experiments measure a larger enhancement than predicted by the classical MD simulations of Jungwirth and Tobias (*10*, *11*).

There are several potential origins of the quantitative difference between our experiments and the simulations. For ease of handling, the experiments were carried out with KBr and KI, whereas the simulations used Na^+ as the cation. We believe that it is highly unlikely that this difference would affect the results. As mentioned previously, we have carried out the experiments at slightly reduced temperatures. In addition, because of the manner in which our experiments are done, the solutions are necessarily at saturation concentration (they are in equilibrium with both water and undissolved solid). The simulations we compare to here were carried out at a concentration of 1.2 M. The salt concentration may affect the amount of anion enhancement observed in the simulations (*10*, *11*). Preliminary results of simulations of more concentrated KBr solutions at –10°C show results that are quite similar to the simulations at 1.2 M shown in Fig. 4 (*23*).

Allen and co-workers (*13*) carried out VSFG experiments on NaBr and NaI solutions at relatively low salt concentrations. However, the disruption of the interfacial hydrogen bonding of the water increased when the salt concentration was increased. Efforts are under way to provide detailed comparisons between the experiments described here and MD simulations carried out for comparable concentrations and temperatures (*23*). In carrying out experiments on solution interfaces, it is impossible to completely avoid contamination of the interface with impurities. As noted above, in our experiments the liquid/vapor interface contains small amounts (submonolayer) of carbonaceous material. An advantage of the XPS experiments is that we can easily quantify the amount of carbonaceous material at the interface. The anion/cation ratios that we measure are insensitive to the small amount of carbon at the interface in the submonolayer regime. Because it is likely that all liquid/vapor interface experiments have small amounts of carbonaceous material at the interface, it is important to quantify these amounts in future experiments and understand the impact on interface properties.

In making quantitative comparisons between experiments and the classical MD simulations, it should also be noted that the detailed results of such simulations are known to be particularly sensitive to the interaction potentials that are used (*24*). Molecular simulations have been successfully tested against and found to be consistent with bulk solution properties and even against the results of cluster studies. However, there are few quantitative results on solution interfaces to provide benchmark tests for the interaction potentials that are used for the study of liquid/vapor interfaces. As a result, it will be very important to continue close collaborative work between new experiments and simulations in this area.

References and Notes

1. E. M. Knipping *et al.*, *Science* **288**, 301 (2000).
2. S. W. Hunt *et al.*, *J. Phys. Chem. A* **108**, 11559 (2004).
3. C. W. Spicer *et al.*, *Nature* **394**, 353 (1998).
4. R. Sander *et al.*, *Atmos. Chem. Phys.* **3**, 1301 (2003).

5. C. W. Spicer *et al.*, *Atmos. Environ.* **36**, 2721 (2002).
6. S. Ghosal, A. Shbeeb, J. C. Hemminger, *Geophys. Res. Lett.* **27**, 1879 (2000).
7. L. A. Barrie *et al.*, *Nature* **334**, 138 (1988).
8. L. A. Barrie, U. Platt, *Tellus* **49B**, 450 (1997).
9. J. H. Hu *et al.*, *J. Phys. Chem.* **99**, 8768 (1995).
10. P. Jungwirth, D. J. Tobias, *J. Phys. Chem. B* **105**, 10468 (2001).
11. P. Jungwirth, D. J. Tobias, *J. Phys. Chem. B* **106**, 6361 (2002).
12. B. C. Garrett, *Science* **303**, 1146 (2004).
13. D. Liu, G. Ma, L. M. Levering, H. C. Allen, *J. Phys. Chem. B* **108**, 2252 (2004).
14. E. A. Raymond, G. L. Richmond, *J. Phys. Chem. B* **108**, 5051 (2004).
15. P. B. Petersen *et al.*, *Chem. Phys. Lett.* **397**, 46 (2004).
16. R. Weber *et al.*, *J. Phys. Chem. B* **108**, 4729 (2004).
17. D. F. Ogletree *et al.*, *Rev. Sci. Instrum.* **73**, 3872 (2002).
18. The experiments were carried out at the Berkeley Advanced Light Source in beamlines 9.3.2 and 11.0.2. Salt crystals ~2 mm thick and ~5 mm² were mounted on a cooled copper substrate. They were cleaved in situ or just before introduction into the vacuum system. Vapor from degassed Milli-Q water (Millipore Corporation, Billerica, MA) was introduced through a leak valve and monitored with a capacitance nanometer absolute pressure gauge.
19. J. J. Yeh, I. Lindau, *At. Data Nuc. Data Tables* **32**, 1 (1985).
20. W. F. Linke, *Solubilities, Inorganic and Metal Organic Compounds: A Compilation of Solubility Data from the Periodical Literature* (Van Nostrand, Princeton, NJ, ed. 4, 1958), vol. 2.
21. The probability that a photoelectron generated below the sample surface will contribute to the well-defined photoelectron peak for an element depends on the IMFP of the electron Γ(KE), which is a function of its kinetic energy. The photoelectron signal predicted from the classical MD simulations is then calculated with the convolution integral $S = \int_0^z e^{\frac{z}{\Gamma(KE)}} \cdot D(z)dz$ where z is the distance into the sample from the vapor/liquid interface and $D(z)$ is the density of the particular element as a function of z from the simulation.
22. C. J. Powell, A. Jablonski, *NIST Electron Inelastic-Mean-Free-Path Database, Version 1.1* (National Institute of Standards and Technology, Gaithersburg, MD, 2000).
23. M. Roeselová, Department of Molecular Modeling, Institute of Organic Chemistry and Biochemistry, Academy of Sciences of the Czech Republic, private communication.
24. L. X. Dang, T. M. Chang, *J. Phys. Chem. B* **106**, 235 (2002).
25. Supported by the Director, Office of Science, Office of Basic Energy Science, U.S. Department of Energy under contract no. DE-AC03-76SD00098 and DE-AC03-76SF00098. J.C.H. and S.G. thank the NSF for support (grants 0080806, 0209719, and 0431312). G.K. thanks the Alexander von Humboldt Foundation for support. F.G.R. thanks the Consejo Nacional de Investigaciones Científicas y Técnicas (Argentina). The authors thank D. Tobias and P. Jungwirth for providing the numerical data from their classical MD simulations of 1.2 M alkali-halide solutions, which were used for comparison with the experiments. We thank M. Roeselová for discussion of the preliminary results of classical MD simulations of higher concentration KBr solutions at –10°C. S.G. and M.S. thank M. Luna for assistance in the initial phase of this project and J. Newberg for help procuring the single-crystal samples. S.G. also thanks H. Liu for experimental help in the initial phase of these experiments. E. Wong's help and expertise with the technical aspects of the experiments are greatly appreciated.

19 October 2004; accepted 15 December 2004
10.1126/science.1106525

Nightglow in the Upper Atmosphere of Mars and Implications for Atmospheric Transport

Jean-Loup Bertaux,[1]* François Leblanc,[1] Séverine Perrier,[1] E. Quemerais,[1] Oleg Korablev,[2] E. Dimarellis,[1] A. Reberac,[1] F. Forget,[3] P. C. Simon,[4] S. A. Stern,[5] Bill Sandel,[6] the SPICAM team†

We detected light emissions in the nightside martian atmosphere with the SPICAM (spectroscopy for the investigation of the characteristics of the atmosphere of Mars) ultraviolet (UV) spectrometer on board the Mars Express. The UV spectrum of this nightglow is composed of hydrogen Lyman α emission (121.6 nanometers) and the γ and δ bands of nitric oxide (NO) (190 to 270 nanometers) produced when N and O atoms combine to produce the NO molecule. N and O atoms are produced by extreme UV photodissociation of O_2, CO_2, and N_2 in the dayside upper atmosphere and transported to the night side. The NO emission is brightest in the winter south polar night because of continuous downward transport of air in this region at night during winter and because of freezing at ground level.

Airglow spectroscopy and radiometry are powerful methods for remote sensing investigations of the physics of upper atmospheres of the terrestrial planets (*1*). For instance, martian dayglow spectra (*2*, *3*) reveal the effect of solar extreme ultraviolet (EUV) radiation on upper atmosphere CO_2 as a major heating mechanism and on production of a ionosphere. On Venus, the observed UV nightglow is composed of weak O emissions, as a signature of electron precipitations capable of maintaining a nighttime ionosphere (*1*), and stronger spectra of O_2 and NO molecules, from radiative recombination of N and O atoms produced on the day side and transported to the night side. Thus, these NO and O_2 emissions are important tracers of atmospheric transport at high altitudes, constraining general circulation models. Up to now, however, nightglow from Mars had escaped detection.

The SPICAM (spectroscopy for the investigation of the characteristics of the atmosphere of Mars) instrument on board Mars Express (MEX) is a UV-infrared (IR) dual spectrometer dedicated primarily to the study of the atmosphere and ionosphere of Mars (*4*, *5*) but also capable of providing important results on the surface albedo of Mars. A UV imaging spectrometer (118 to 320 nm, spectral resolution of 1.5 nm, intensified charge coupled device) is dedicated to nadir viewing, limb viewing, and atmospheric vertical profiling by stellar and solar occultations (*6*).

The UV channel of SPICAM is a full UV imaging spectrometer that spatially resolves 288 spectra along its slit, but, because of telemetry constraints, only five spectra can be transmitted for each 1-s measurement. These spectra are usually a sum of n individual spectra, with $n = 32$ in the present case, forming five band spectra (numbered from 0 to 4). The slit of the spectrometer, placed at the focus of the parabolic mirror, has two parts: a narrow part, achieving a spectral resolution of 1.5 nm, and a wide part, achieving a higher (10 times greater) photometric sensitivity for extended sources at the expense of a reduced spectral resolution (6 nm). Two band spectra were acquired with the narrow slit, and three band spectra with the wide slit, during each second in the observations reported here (*7*).

At the time of this observation [orbit 734, 16 August 2004, 07:00 universal time (UT)], the orbit of MEX had its pericenter on the night side, at an altitude of 266 km and a latitude of –16°. The orbit is almost polar, and MEX was descending from north to south. The attitude was fixed in an inertial system (departing from the usual nadir pointing near pericenter), so that the line of sight (LOS), which is aligned with the + Z body axis of the spacecraft, provided a grazing view of the limb while MEX was passing through its pericenter (±10 mn). As a result, the altitude of the tangent point of the LOS [Mars nearest point (MNP)] changed from 375 km to a minimum of 15 km and back to 422 km. At the same time, the latitude changed from –11° to –70°. The whole

[1]Service d'Aéronomie du CNRS/Institut Pierre-Simon Laplace (IPSL), BP.3, 91371, Verrières-le-Buisson, France. [2]Space Research Institute (IKI), 84/32 Profsoyuznaya, 117810 Moscow, Russia. [3]Laboratoire de Météorologie Dynamique/IPSL, University Paris 6, 75252 Paris, France. [4]Belgian Institute for Space Aeronomy (BIRA), 3 Avenue Circulaire, B-1180 Brussels, Belgium. [5]Southwest Research Institute, Boulder, CO 80302, USA. [6]Lunar and Planetary Laboratory, 1541 East University Boulevard, University of Arizona, Tucson, AZ 85721, USA.

*To whom correspondence should be addressed. E-mail: bertaux@aerov.jussieu.fr
†Members of the SPICAM team and their affiliations are listed at the end of the References and Notes.